

Metoda robnih elementov za dinamiko viskoelastične Maxwellove tekočine

The Boundary-Element Method for the Dynamics of a Viscoelastic Maxwell Fluid

Leopold Škerget - Matej Požarnik

V prispevku je prikazan razvoj numerične sheme na osnovi metode robnih elementov (MRE) za modeliranje ravinskih tokov viskoelastične tekočine. Kot podlaga za razvoj je namenjena shema za modeliranje nestisljivih viskoznih tokov, ki smo jo razširili in ji dodali potrebne člene za zajemanje viskoelastičnosti neneutonskih tekočin. Posebno pozornost smo namenili integraciji ohranitvenih zakonov in reoloških modelov. Shema je zapisana za hitrostno-vrtinčno formulacijo vodilnih enačb. Kot testni primeri so predstavljeni tokovi neneutonske Maxwellove tekočine v kanalih različnih geometrijskih oblik.

© 2002 Strojniški vestnik. Vse pravice pridržane.

(Ključne besede: modeli robnih elementov, dinamika tekočin, tekočine viskoelastične, modeli Maxwellovi)

In this paper we show a numerical scheme based on the boundary-element method (BEM) for the numerical modeling of planar, viscoelastic fluid flows. In particular, the singular-boundary-integral approach, which has been established for the viscous, incompressible flow problem, is modified and extended to include the viscoelastic fluid state. Special attention is given to a proper integration of the conservation and constitutive equations. A velocity-vorticity formulation of the governing equations is adopted. As test cases, non-Newtonian–Maxwell fluid flows in the channels of various geometries are studied.

© 2002 Journal of Mechanical Engineering. All rights reserved.

(Keywords: boundary element methods, fluid dynamics, viscoelastic fluids, Maxwell models)

0 UVOD

V prispevku predstavljamo numerični model robnih elementov (MRE) za reševanje dinamike viskoelastične nestisljive tekočine. Sistem Navier-Stokesovih enačb ob upoštevanju Maxwellovih modelov tečenja viskoelastične tekočine smo zapisali za hitrostno-vrtinčno formulacijo. Ta ima v primeru robnoobmočne integralske predstavitev vodilnih enačb določene prednosti, saj smo iz računske sheme izločili tlak, kar pomeni, da se izognemo težavam pri predpisovanju robnih vrednosti tlaka. Posebna pozornost je posvečena spremembam diferencialnih vodilnih enačb v pripadajoče robnoobmočne integralske predstavitev, ki zadoščajo omejitvenemu kriteriju ohranitve mase ozziroma pogoju solenoidnosti tokovnega polja.

Stabilnost in natančnost numeričnega algoritma dosežemo brez dodatnih stabilizacijskih tehnik z uporabo parabolične difuzijske osnovne rešitve, ki opisuje linearni del prenosnega pojava. Numerični model, predstavljen v prispevku, je mogoče nadgraditi

0 INTRODUCTION

This paper deals with a numerical scheme based on the boundary-element method (BEM) developed to numerically simulate viscoelastic, incompressible fluid flows. The method is based on a solution of the Navier-Stokes equations set in the velocity-vorticity formulation for different viscoelastic Maxwell fluids. This formulation has some advantages in the case of a boundary-domain integral representation of governing equations. It is simpler than a primitive variable formulation since the pressure does not appear explicitly in the field-function equations and thus the well-known difficulty connected with the computation of the pressure boundary values in incompressible flows is avoided. Particular attention is given to a proper transformation of the differential governing equations to the corresponding boundary-domain integral representations that satisfy the continuity equation or the solenoidality of the velocity field exactly.

The stability and the accuracy of the developed numerical scheme is achieved by employing the parabolic diffusion fundamental solution describing the linear part of transport phenomena without any additional stabilization techniques. The numerical model presented here is easy to upgrade in the sense of effectiveness,

v smislu učinkovitosti, stabilnosti in natančnosti z uporabo difuzivno-konvektivne osnovne rešitve, ki zajema večji del prenosnega pojava, in modela podobmočij [5].

1 VODILNE ENAČBE

1.1 Ohranitveni zakoni

Analitični opis gibanja zvezne snovi temelji na osnovnih ohranitvenih zakonih mase, gibalne količine, energije in kemijskih sestavin, pripadajočih reoloških modelih in enačbah stanja. V obravnavi se bomo omejili na laminarni tok nestisljive viskoelastične izotropne tekočine v območju rešitve Ω , ograjenim z ograjo Γ .

Opozovane funkcije polja so vektor hitrosti $v_i(r_j, t)$, tlak $p(r_j, t)$ in temperaturno polje $T(r_j, t)$, ki zadoščajo kontinuitetni, gibalni in energijski enačbi:

$$\frac{\partial v_j}{\partial x_j} = 0 \quad (1)$$

$$\rho_0 \frac{Dv_i}{Dt} = \frac{\partial \sigma_{ij}}{\partial x_j} + \rho g_i \quad (2)$$

$$c_{p0} \rho_0 \frac{DT}{Dt} = -\frac{\partial q_j}{\partial x_j} + I \quad (3)$$

ki so zapisane v obliki kartezičnega tenzorskega zapisa x_i in kjer so ρ_0 in c_{p0} nespremenljiva masna gostota oziroma izobarna specifična toplota, t čas, g_i težnostni pospešek, σ_{ij} napetostni tenzor, q_j gostota difuzijskega toplotnega toka in $D(\cdot)/Dt = \partial(\cdot)/\partial t + v_k \partial(\cdot)/\partial x_k$ Stokesov oziroma snovski odvod spremenljivke (\cdot) . V gibalni enačbi (2) smo upoštevali nestisljivost tekočine v smislu Boussinesqove poenostavitev, pri kateri je vpliv spremenljive masne gostote zajet le v prostorninski sili ρg_i .

Zapisani sistem ohranitvenih enačb pomeni nedokončan sistem parcialnih diferencialnih enačb, ki ga moramo dopolniti z ustreznimi reološkimi modeli oziroma modeli tečenja za posamezno tekočino in znanimi robnimi ter začetnimi pogoji. Ti so v splošnem odvisni od zapisanega sistema enačb in so lahko podani za osnovne fizikalne ali izpeljane funkcije polja.

1.2 Reološki modeli

Cauchyjev napetostni tenzor σ_{ij} lahko v primeru toka nestisljive tekočine ločimo na prispevek tlaka in dodatnega deviatoričnega napetostnega tenzorja τ_{ij} :

$$\sigma_{ij} = -p\delta_{ij} + \tau_{ij} \quad (4)$$

kjer je δ_{ij} Kroneckerjeva funkcija delta. Bistveni del dinamike viskoelastičnih tekočin je izbira primerenega reološkega modela, ki podaja soodvisnost dodatnih

stability and accuracy using a diffusion-convective fundamental solution where a larger part of the transport phenomena is taken into account. The subdomain technique can also be implemented [5].

1 GOVERNING EQUATIONS

1.1 Conservation laws

The analytical description of the motion of a continuous medium is based on the conservation of mass, momentum, energy and species concentration, with associated rheological models and equations of state. The present development will be focused on the laminar flow of an incompressible, viscoelastic, isotropic fluid in a solution domain Ω bounded by a boundary Γ .

The field functions of interest are the velocity vector field $v_i(r_j, t)$, the pressure field $p(r_j, t)$, and the temperature field $T(r_j, t)$, such that the mass, momentum, and energy equations:

$$\frac{\partial v_j}{\partial x_j} = 0 \quad (1)$$

$$\rho_0 \frac{Dv_i}{Dt} = \frac{\partial \sigma_{ij}}{\partial x_j} + \rho g_i \quad (2)$$

$$c_{p0} \rho_0 \frac{DT}{Dt} = -\frac{\partial q_j}{\partial x_j} + I \quad (3)$$

written in the Cartesian frame x_i are satisfied, where ρ_0 and c_{p0} are the constant fluid mass density and the isobaric specific heat capacity, t is the time, g_i is the gravitational acceleration vector, σ_{ij} denotes the components of the total stress tensor, q_j stands for the specific heat flux, and $D(\cdot)/Dt = \partial(\cdot)/\partial t + v_k \partial(\cdot)/\partial x_k$ represents the Stokes material derivative of the variable (\cdot) . The natural convection effect is considered in the momentum, Eq. (2), by using the Boussinesq approximation, where the temperature's influence on mass density is considered only with the body force ρg_i .

The set of field equations needs to be closed and solved in conjunction with the appropriate rheological equations of the fluid and the boundary, and the initial conditions of the flow problem. The boundary conditions in general depend on the dependent variables applied, i.e. the primitive or velocity-vorticity variables formulation.

1.2 Rheological models

For an incompressible fluid the Cauchy total stress σ_{ij} can be decomposed into a pressure contribution plus an extra deviatoric stress-tensor field function τ_{ij} :

where δ_{ij} is the Kronecker delta. The central problem in visco-elastic fluid dynamics is the selection of an appropriate rheological model that relates the extra

napetosti v en. (4) in kinematike toka. Obravnavo bomo omejili na razmeroma preproste diferencialne konstitutivne enačbe, znane kot implicitni Maxwellovi reološki modeli. Za širok spekter snovi, kakor so na primer tekočine s pojmemajocim spominom, lahko konstitutivne enačbe zapišemo v obliki odvisnosti med napetostnim in deformacijskim tenzorjem ter njuniimi odvodi po času.

Za Eulerjev postopek velja, da lahko snovske časovne odvode poljubnega simetričnega tenzorja drugega reda u_{ij} , ki ga lahko enačimo z dodatnim napetostnim tenzorjem τ_{ij} ali deformacijskim tenzorjem $\dot{\epsilon}_{ij}$, podamo na različne načine. Z naslednjim izrazom definiramo Stokesov časovni snovski odvod tenzorja:

$$\frac{Du_{ij}}{Dt} = \frac{\partial u_{ij}}{\partial t} + v_k \frac{\partial u_{ij}}{\partial x_k} \quad (5)$$

nato zgornje konvektivni oziroma sodeformabilni:

$$\overset{\nabla}{u}_{ij} = \frac{Du_{ij}}{Dt} - u_{ik} L_{jk} - u_{jk} L_{ik} \quad (6)$$

medtem ko je spodnje konvektivni odvod podan z izrazom:

$$\overset{\Delta}{u}_{ij} = \frac{Du_{ij}}{Dt} + u_{ik} L_{kj} + u_{jk} L_{ki} \quad (7)$$

kjer nadpisa ∇ in Δ označuje zgornje oziroma spodnje konvektivni odvod. Hitrostni gradient L_{ij} je definiran kot:

$$L_{ij} = \frac{\partial v_i}{\partial x_j} = \dot{\epsilon}_{ij} + \dot{\Omega}_{ij} \quad (8)$$

kjer je $\dot{\Omega}_{ij}$ tenzor vrtilnih hitrosti.

Pri implicitnih Maxwellovih reoloških modelih podamo dodatni napetostni tenzor z vsoto viskoznih in elastičnih učinkov:

$$\tau_{ij} = \tau_{ij}^v + \tau_{ij}^e \quad (9)$$

Linearni Maxwellov konstitutivni model podamo z odvisnostjo:

$$\tau_{ij} = 2\eta_0 \dot{\epsilon}_{ij} - \lambda_1 \frac{\partial \tau_{ij}}{\partial t} \quad (10)$$

kjer snovska stalnica tekočine λ_1 pomeni napetostni sprostitevni čas, medtem ko je η_0 dinamična viskoznost. Vpliv elastičnosti, ki je podan z lokalnim časovnim odvodom dodatnega napetostnega tenzorja, je pomemben le med prehodnim pojavom. Z razvojem hitrostnega polja lokalni časovni odvod izgublja pomembnost, tako da v ustaljenem stanju prevladujejo učinki viskoznosti.

Najpreprostejši kvazilinearen Maxwellov model, podan v obliki:

$$\tau_{ij} = 2\eta_0 \dot{\epsilon}_{ij} - \lambda_1 \frac{D\tau_{ij}}{Dt} \quad (11)$$

zajema nelinearnost zaradi lokalnega in konvektivnega odvoda napetostnega tenzorja.

stress in Eq. (4) to the flow kinematics. The differential constitutive equations to be considered here are implicit, rate-type rheological models, generally associated with the name of Maxwell. For the broad class of materials, such as simple fluids with fading memory, the constitutive equation can be expressed using a relation between stress and the strain-rate tensor and their time derivatives.

For an Eulerian reference frame the material time derivative or convected derivative of an arbitrary symmetric, second-order tensor u_{ij} , which can be equated to the extra-stress tensor τ_{ij} or the strain-rate tensor $\dot{\epsilon}_{ij}$, can be formulated in several ways. Let us first define the Stokes material time derivative with the expression:

then the upper-convected or codeformation:

while the lower-convected derivative is defined as:

where the superscripts ∇ and Δ stand for the upper- or lower-convected derivatives, respectively, and the velocity-gradient tensor L_{ij} is defined as:

where $\dot{\Omega}_{ij}$ denotes the rotational velocity tensor.

Using implicit Maxwell rheological models the extra-stress tensor is given as a sum of the viscosity and elasticity effects:

The linear Maxwell constitutive model is given as follows:

where λ_1 is a material constant for the fluid and is called the stress-relaxation time, whereas η_0 stands for the dynamic viscosity. The elasticity is given by the local time derivative of the additional stress tensor, which is significant during transient conditions. As the flow develops, the local time derivative losses its influence to finally arrive at a steady state where the viscosity is dominant.

The simplest quasilinear Maxwell model may be given in the following form:

where the nonlinearity of the model is due to the local and convective derivatives of the stress tensor.

Model predstavljen z en. (11), v praksi ni uporaben, kljub temu pa ga zaradi preprostosti lahko uporabimo pri študiju stabilnosti in natančnosti razvitega numeričnega algoritma.

V nadaljevanju sta prikazana oba konvektivna Maxwellova modela. Zgornje konvektivni Maxwellov model podamo z odvisnostjo:

$$\tau_{ij} = 2\eta_0 \dot{\epsilon}_{ij} - \lambda_1 \overset{\triangledown}{\tau}_{ij} \quad (12)$$

medtem ko za spodnje konvektivni model velja zapis:

$$\tau_{ij} = 2\eta_0 \dot{\epsilon}_{ij} - \lambda_1 \overset{\Delta}{\tau}_{ij} \quad (13)$$

Zgornje konvektivni Maxwellov model je namenjen testiranju numeričnih modelov reševanja viskoelastičnih tokov, saj je gibanje nekaterih stvarnih tekočin, vsaj v omejenem obsegu, mogoče opisati z en. (12).

Preostane še, da zapišemo konstitutivni model difuzijskega topotnega toka v en. (3). V primeru intenzivnega prehodnega pojava prenosa toplote moramo upoštevati končno hitrost širjenja motnje, tako da velja odvisnost:

$$q_i = -k_0 \frac{\partial T}{\partial x_i} - \lambda_0 \frac{\partial q_i}{\partial t} \quad (14)$$

kjer sta snovski stalnici k_0 in λ_0 topotna prevodnost in topotni sprostitveni čas. Za večino praktično pomembnih prenosnih pojavov zadošča poenostavitev, znana kot Fourierjev zakon difuzije toplote:

$$q_i = -k \frac{\partial T}{\partial x_i} \quad (15)$$

1.3 Povzetek vodilnih enačb

Z upoštevanjem konstitutivnih modelov za napetostni tenzor (9) do (13) in gostoto topotnega toka (15) v ohranitvenih zakonih (2) in (3) izpeljemo naslednji sistem nelinearnih enačb:

$$\frac{\partial v_j}{\partial x_j} = 0 \quad (16)$$

$$\rho_0 \frac{Dv_i}{Dt} = -\frac{\partial p}{\partial x_i} + \eta_0 \frac{\partial^2 v_i}{\partial x_j \partial x_j} + \rho g_i + \frac{\partial \tau_{ij}^e}{\partial x_j} \quad (17)$$

$$\tau_{ij} = 2\eta_0 \dot{\epsilon}_{ij} + \tau_{ij}^e \quad (18)$$

$$\frac{\partial T}{\partial t} = a_0 \frac{\partial^2 T}{\partial x_j \partial x_j} + \frac{I}{c_{p0} \rho_0} \quad (19)$$

kjer je $a_0 = k_0 / c_{p0} \rho_0$ topotna difuzivnost. Sklenjen sistem enačb (16) do (19) je formalno identičen enačbam, ki opisujejo tok newtonske viskozne tekočine z izjemo dodatnega člena, ki je posledica elastičnih učinkov tekočine in je v sistemu označen z nadpisom "e". Ta člen v enačbi ohranitve gibalne

The model (11) does not relate to practical problems, but it can be examined due to its simplicity as an appropriate model to study the stability and accuracy of the developed numerical solution algorithm.

In addition, both convected Maxwell models are studied. The upper-convected Maxwell model is governed by the following constitutive relation:

while for the lower-convected Maxwell model the following equation is valid:

The upper-convected Maxwell model (12) is used extensively in testing numerical solution models. Some real fluids behave qualitatively like Eq. (12), at least over a limited range of kinematics.

Let us write the constitutive model of diffusion heat flux in Eq. (3). In the case of intensive, unsteady heat transfer it is important to take into account the terminal velocity of a moving frontier:

where the material constants k_0 and λ_0 stand for the heat conductivity and the heat relaxation time. For most heat-transfer problems of practical importance the simplification known as the Fourier law of heat diffusion is accurate enough:

1.3 Summary of the governing equations

Combining the constitutive models for the stress tensor (9) to (13) and the specific heat flux (15) in the conservation equations (2) and (3), the following system of nonlinear equations is developed:

where $a_0 = k_0 / c_{p0} \rho_0$ is the thermal diffusivity. The closed system of equations (16) to (19) is formally identical to the equations governing the motion of a Newtonian viscous fluid, except for the additional term describing the elasticity effects (denoted by the superscript "e"). The appearance of the additional terms

količine vpelje dodatno nelinearnost v dinamični sistem enačb.

Za tok v ravnini sistem enačb od (16) do (19) zagotavlja sedem enačb za sedem neznank, $v_1, v_2, p, \tau_{11}, \tau_{12}, \tau_{22}$, in T . Enačbe razrešimo z upoštevanjem primernih robnih in začetnih pogojev. Če predpostavimo, da so vse funkcije polja, npr. $v_i^n = v_i^n(r_j, t)$, $\tau_{ij}^n = \tau_{ij}^n(r_j, t)$ itd., v časovnem koraku $t = t_n$ znane, je treba določiti vrednosti funkcij polja v naslednjem trenutku $t_{n+1} = t_n + \Delta t$.

2 HITROSTNO-VRTINČNA FORMULACIJA

Z vektorjem vrtinčnosti $\omega_i(r_j, t)$, ki pomeni rotor hitrostnega polja $v_i(r_j, t)$:

$$\omega_i = e_{ijk} \frac{\partial v_k}{\partial x_j},$$

računsko shemo gibanja tekočine razdelimo na kinematični in kinetični del [8]. Kinetiko toka podamo z nelinearno parabolično difuzivno-konvektivno prenosno enačbo vrtinčnosti, ki jo izpeljemo z delovanjem operatorja rotor na gibalno enačbo (17):

$$\frac{D\omega_i}{Dt} = \frac{\partial \omega_i}{\partial t} + v_j \frac{\partial \omega_i}{\partial x_j} = v_0 \frac{\partial^2 \omega_i}{\partial x_j \partial x_j} + \omega_j \frac{\partial v_i}{\partial x_j} + \frac{1}{\rho_0} e_{ijk} g_k \frac{\partial \rho}{\partial x_j} + \frac{1}{\rho_0} e_{ijk} \frac{\partial^2 \tau_{km}^e}{\partial x_j \partial x_k} \quad (21)$$

za $i,j,k,m = 1,2,3$. V prenosni enačbi (21) je opazen dodatni prenosni člen $\omega_j L_{ij}$, ki ga ne zasledimo v gibalni enačbi (17). Z upoštevanjem odvisnosti:

$$\omega_j L_{ij} = \omega_j (\dot{\epsilon}_{ij} + \dot{\Omega}_{ij}) = \omega_j \dot{\epsilon}_{ij} \quad (22)$$

preprosto pokažemo, da del člena $\omega_j \dot{\epsilon}_{ij}$, $\dot{\epsilon}_{ij}$ za $i = j$, opravlja prenos vrtinčnosti z raztezanjem vrtinčne črte, preostali del, $\dot{\epsilon}_{ij}$ za $i \neq j$, pa prenaša vrtinčnost z obračanjem vrtinčne črte. Prenosni pojav raztezanja in obračanja ne obstaja pri ravninskih tokovih, ko se vektorska enačba (21) poenostavi v skalarno:

$$\frac{D\omega}{Dt} = \frac{\partial \omega}{\partial t} + v_j \frac{\partial \omega}{\partial x_j} = v_0 \frac{\partial^2 \omega}{\partial x_j \partial x_j} + \frac{1}{\rho_0} e_{ij} g_j \frac{\partial \rho}{\partial x_i} + \frac{1}{\rho_0} e_{ij} \frac{\partial^2 \tau_{jk}^e}{\partial x_i \partial x_k} \quad (23)$$

za $i,j,k = 1,2$. Enačba (21) podaja časovno sprememblo vrtinčnosti delca tekočine zaradi viskozne difuzije, konvekcije, vzgona, učinkov deformacije in elastičnosti tekočine. V primerjavi z enačbo gibanja newtonske viskozne tekočine je enačba (21) močnejše nelinearna, prav zaradi močno nelinearnega elastičnega izvirnega člena.

Z delovanjem operatorja rotor na vektor vrtinčnosti:

$$\vec{\nabla} \times \vec{\omega} = \vec{\nabla} \times (\vec{\nabla} \times \vec{v}) = \vec{\nabla}(\vec{\nabla} \cdot \vec{v}) - \Delta \vec{v} \quad (24)$$

in ob upoštevanju kontinuitetne enačbe (16), $\operatorname{div} \vec{v} = 0$, izpeljemo naslednjo vektorsko eliptično Poissonovo enačbo:

in the momentum equation at the same time increases the nonlinearity of the dynamical system of equations.

For the two-dimensional planar geometry the Eqs. (16) to (19) provide seven relations for the seven unknowns, $v_1, v_2, p, \tau_{11}, \tau_{12}, \tau_{22}$, and T . The above field equations are to be solved for the appropriate boundary and initial conditions. Assuming that at time level $t = t_n$ all the relevant field quantities, such as $v_i^n = v_i^n(r_j, t)$, $\tau_{ij}^n = \tau_{ij}^n(r_j, t)$, etc., are known, the issue is to determine the field functions during the time level $t_{n+1} = t_n + \Delta t$.

2 THE VELOCITY-VORTICITY FORMULATION

Introducing the vorticity vector field function $\omega(r_j, t)$ as a curl of the corresponding velocity field $v_i(r_j, t)$:

$$\frac{\partial \omega_j}{\partial x_j} = 0 \quad (20)$$

which is a solenoidal vector by definition, the fluid-motion computation procedure is partitioned into its kinetics and kinematics [8] parts. The vorticity transport in the fluid domain is governed by a nonlinear parabolic diffusion-convection equation obtained as a curl of the momentum eq. (17):

$$\frac{\partial v_i}{\partial x_j} + \frac{1}{\rho_0} e_{ijk} g_k \frac{\partial \rho}{\partial x_j} + \frac{1}{\rho_0} e_{ijk} \frac{\partial^2 \tau_{km}^e}{\partial x_j \partial x_k} \quad (21)$$

for $i,j,k,m = 1,2,3$. In the transport eq. (21) an additional transport term $\omega_j L_{ij}$ is represented, whereas it cannot be found in eq. (17). Regarding the relation:

it is easy to understand the behaviour of $\omega_j \dot{\epsilon}_{ij}$, $\dot{\epsilon}_{ij}$ for $i = j$, representing vorticity transport due to the stretching of the vorticity line, while the other part, $\dot{\epsilon}_{ij}$ for $i \neq j$, stands for the twisting of the vorticity line. Twisting and stretching transport phenomena do not exist during the planar flows when vector eq. (21) is reduced to the scalar one:

for $i,j,k = 1,2$. The vorticity equation (21) expresses time-dependent vorticity transport by viscous diffusion, convection, buoyancy forces, while the elasticity and deformation of the fluid acts as a highly nonlinear production term, making the nonlinearity of the equation even more severe, when compared to Newtonian viscous fluid flow.

By applying the curl operator to the vorticity definition:

and by using the continuity eq. (16), $\operatorname{div} \vec{v} = 0$, the following vector elliptic Poisson equation is obtained:

$$\frac{\partial^2 v_i}{\partial x_j \partial x_j} + e_{ijk} \frac{\partial \omega_k}{\partial x_j} = 0 \quad (25)$$

Enačba podaja kinematiko toka nestisljive tekočine oziroma združljivosti in omejitveni pogoj med solenoidnima vektorskima poljema hitrosti in vrtinčnosti v dani točki prostora in časa. Z namenom, da bi povečali konvergenco in stabilnosti vezane hitrostno-vrtinčne iterativne sheme, en. (25) zapišemo v njeni nepravi prehodni obliku, kar se izraža v naslednji parabolični difuzijski enačbi za vektor hitrosti

$$\frac{\partial^2 v_i}{\partial x_j \partial x_j} - \frac{1}{\alpha} \frac{\partial v_i}{\partial t} + e_{ijk} \frac{\partial \omega_k}{\partial x_j} = 0 \quad (26)$$

kjer je α sprostivni parameter. Očitno je, da je vodilna hitrostna enačba (26) natančno izpolnjena v ustaljenem stanju ($t \rightarrow \infty$), ko umetni časovni odvod hitrosti odpade.

3 TLAČNA ENAČBA

Za nestisljive tekočine velja ugotovitev, da je tlak le funkcija hitrostnega polja in nasprotno, medtem ko je gostota nespremenljiva. Tlak torej ni termodinamična veličina stanja. Zapišimo gibalno en. (17) z upoštevanjem vektorske enakosti (24) za tlačni gradient $\text{grad } p$:

$$\frac{\partial p}{\partial x_i} = f_i = -\rho_0 \frac{Dv_i}{Dt} - \eta_0 e_{ijk} \frac{\partial \omega_k}{\partial x_j} + \rho g_i + \frac{\partial \tau_{ij}^e}{\partial x_j} \quad (27)$$

ki se v primeru ravninskega toka poenostavi v odvisnost:

$$\frac{\partial p}{\partial x_i} = f_i = -\rho_0 \frac{Dv_i}{Dt} - \eta_0 e_{ij} \frac{\partial \omega}{\partial x_j} + \rho g_i + \frac{\partial \tau_{ij}^e}{\partial x_j} \quad (28)$$

V vektorski funkciji f_i smo združili vztrajnostne, difuzijske, težnostne in elastične učinke. Pri izpeljavi tlačne enačbe v odvisnosti od hitrosti poiščemo divergenco členov en. (27), kar se kaže v naslednji eliptični Poissonovi enačbi za tlak:

$$\frac{\partial p}{\partial x_i \partial x_i} - \frac{\partial f_i}{\partial x_i} = 0 \quad (29)$$

4 METODA ROBNIH ELEMENTOV

Uporaba Greenovih osnovnih rešitev kot utežnih funkcij v numeričnem modelu pomeni eno izmed osnovnih lastnosti in prednosti metode robnih elementov (MRE). Ker osnovne rešitve opisujejo le linearni del prenosnega pojava, je izbira primerenega linearnega operatorja $L[\cdot]$ ključnega pomena za zapis integralskih enačb, ki ustrezajo prvotnemu sistemu ohranitvenih diferencialnih enačb.

Znane diferencialne modele prenosnih pojavov v toku tekočine lahko zapišemo v obliki naslednjega splošnega stavka:

$$L[u] + b = 0 \quad (30)$$

The equation represents the kinematics of an incompressible fluid motion expressing the compatibility and restriction conditions between the solenoidal velocity and the vorticity vector field functions at a given point in space and time. To accelerate convergence of the coupled velocity-vorticity iterative scheme the false transient approach is used. Thus, in a solution scheme Eq. (25) is rewritten as parabolic diffusion equation for the velocity vector:

with α as a relaxation parameter. It is obvious that the governing velocity equation (26) is exactly satisfied only during the steady state ($t \rightarrow \infty$), when the time derivative vanishes.

3 PRESSURE EQUATION

In the case of incompressible fluid motion, pressure is only a function of the velocity field, and vice versa, while the fluid mass density is assumed to be invariant. Therefore, pressure is not a thermodynamic variable. Let us write momentum, Eq. (17), for the pressure gradient, $\text{grad } p$, by taking into account the vector relation (24):

Inertia, diffusion, gravitational and elasticity effects are incorporated in vector function f_i . To derive the pressure equation dependent on velocity the divergence of Eq. (27) should be calculated, resulting in the elliptic Poisson pressure equation

4 THE BOUNDARY-ELEMENT METHOD

The unique advantage of the boundary-element method (BEM) originates from the application of Green fundamental solutions as particular weighting functions. Since they only consider the linear transport phenomenon, the appropriate selection of a linear differential operator $L[\cdot]$ is of vital importance in establishing stable and accurate singular integral representations corresponding to original differential conservation equations.

All the various conservation models can be written in the following general form

kjer je $L[\cdot]$ eliptični ali parabolični linearni diferencialni operator, $u(r_j, t)$ je poljubna funkcija polja in $b(r_j, t)$ pomeni nehomogeni del nelinearnih vplivov oziroma prostorninskih virov.

4.1 Integralska predstavitev kinematike

Hitrostno en. (26) lahko prepoznamo kot parabolično difuzijsko enačbo, zato uporabimo linearni parabolični difuzijski operator:

$$L[\cdot] = \alpha \frac{\partial^2(\cdot)}{\partial x_j \partial x_j} - \frac{\partial(\cdot)}{\partial t} \quad (31)$$

tako, da lahko zapišemo:

$$L[v_i] + b_i = \alpha \frac{\partial^2 v_i}{\partial x_j \partial x_j} - \frac{\partial v_i}{\partial t} + b_i = 0 \quad (32)$$

Pri izpeljavi singularne robne integralske enačbe izhajamo iz Greenovih teoremov za skalarna polja ali iz integrala utežnega ostanka, kar se kaže v naslednji obliki vektorske integralske formulacije:

$$c(\xi)v_i(\xi, t_F) + \alpha \int_{\Gamma} \int_{t_{F-1}}^{t_F} v_i \frac{\partial u^*}{\partial n} dt d\Gamma = \alpha \int_{\Gamma} \int_{t_{F-1}}^{t_F} \frac{\partial v_i}{\partial n} u^* dt d\Gamma + \int_{\Omega} \int_{t_{F-1}}^{t_F} bu^* dt d\Omega + \int_{\Omega} v_{i,F-1} u_{F-1}^* d\Omega \quad (33)$$

kjer je u^* parabolična difuzijska osnovna rešitev, npr. rešitev enačbe:

$$a \frac{\partial^2 u^*}{\partial x_j \partial x_j} + \frac{\partial u^*}{\partial t} + \delta(\xi, s)\delta(t_F, t) = 0 \quad (34)$$

in podana z izrazom:

$$u^* = \frac{1}{(4\pi a\tau)^{d/2}} \exp\left(-\frac{r^2}{4a\tau}\right) \quad (35)$$

kjer sta (ξ, t_F) in (s, t) izvirna točka in referenčna točka polja, d pomeni izmero problema in $\tau = t_F - t$. Če izenačimo prostorninske sile z enakostjo:

$$b = \alpha e_{ijk} \frac{\partial \omega_k}{\partial x_j} \quad (36)$$

velja končna oblika integralske predstavitev kinematike toka, npr. v vektorski obliki:

$$\begin{aligned} c(\xi)\vec{v}(\xi, t_F) + \alpha \int_{\Gamma} \int_{t_{F-1}}^{t_F} \vec{v} \frac{\partial u^*}{\partial n} dt d\Gamma &= \alpha \int_{\Gamma} \int_{t_{F-1}}^{t_F} \frac{\partial \vec{v}}{\partial n} u^* dt d\Gamma - \alpha \int_{\Gamma} \int_{t_{F-1}}^{t_F} \vec{\omega} \times \vec{n} u^* dt d\Gamma \\ &\quad + \alpha \int_{\Omega} \int_{t_{F-1}}^{t_F} \vec{\omega} \times \vec{\nabla} u^* dt d\Omega + \int_{\Omega} \vec{v}_{F-1} u_{F-1}^* d\Omega \end{aligned} \quad (37)$$

ozioroma v tenzorskem simbolnem zapisu:

$$\begin{aligned} c(\xi)v_i(\xi, t_F) + \alpha \int_{\Gamma} \int_{t_{F-1}}^{t_F} v_i \frac{\partial u^*}{\partial n} dt d\Gamma &= \alpha \int_{\Gamma} \int_{t_{F-1}}^{t_F} \frac{\partial v_i}{\partial n} u^* dt d\Gamma \\ - \alpha e_{ijk} \int_{\Gamma} \int_{t_{F-1}}^{t_F} \omega_j n_k u^* dt d\Gamma + \alpha e_{ijk} \int_{\Omega} \int_{t_{F-1}}^{t_F} \omega_j \frac{\partial u^*}{\partial x_k} dt d\Omega &+ \int_{\Omega} v_{i,F-1} u_{F-1}^* d\Omega \end{aligned} \quad (38)$$

Kinematika ravninskega toka je podana z dvema skalarima enačbama:

$$\begin{aligned} c(\xi)v_i(\xi, t_F) + \alpha \int_{\Gamma} \int_{t_{F-1}}^{t_F} v_i \frac{\partial u^*}{\partial n} dt d\Gamma &= \alpha \int_{\Gamma} \int_{t_{F-1}}^{t_F} \frac{\partial v_i}{\partial n} u^* dt d\Gamma \\ + \alpha e_{ij} \int_{\Gamma} \int_{t_{F-1}}^{t_F} \omega n_j u^* dt d\Gamma - \alpha e_{ij} \int_{\Omega} \int_{t_{F-1}}^{t_F} \omega \frac{\partial u^*}{\partial x_j} dt d\Omega &+ \int_{\Omega} v_{i,F-1} u_{F-1}^* d\Omega \end{aligned} \quad (39)$$

where the operator $L[\cdot]$ can be either elliptic or parabolic, $u(r_j, t)$ is an arbitrary field function, and the nonhomogenous term $b(r_j, t)$ is applied for nonlinear transport effects or pseudo body forces.

4.1 Integral representation of flow kinematics

The velocity Eq. (26) can be recognized as a parabolic diffusion equation. Employing the linear parabolic diffusion operator as follows:

the following can be stated:

The singular boundary integral representation for the velocity vector can be formulated by using the Green theorems for scalar functions or weighting residuals technique rendering the following vector integral formulation:

with u^* the parabolic diffusion fundamental solution as the solution of the equation:

and given by the expression:

where (ξ, t_F) and (s, t) are the source point and the reference field point, d is the dimension of the problem and $\tau = t_F - t$. The pseudo-body force vector includes the vortical fluid flow part:

$$b = \alpha e_{ijk} \frac{\partial \omega_k}{\partial x_j} \quad (36)$$

rendering the following final integral formulation of flow kinematics, in vector form:

or in tensor symbolic notation:

The kinematics of plane motion is given by two scalar equations as follows:

Eno osnovnih izhodišč numeričnega modela toka nestisljive tekočine je divergence prosta oziroma solenoidna rešitev za hitrostno in vrtinčno polje. Za en. (36) oziroma (38) lahko preprosto pokažemo, da sta enačbi izpoljeni tudi v primeru, ko nobena od divergenc ni enaka nič [9]. Povzamemo lahko, da en. (38) v splošnem ne predstavlja kinematike toka nestisljive tekočine. S ponovno zahtevo po združljivosti in omejitvi hitrostnega ter vrtinčnega polja, $\vec{\omega} = \text{rot } \vec{v}$ in $\text{div } \vec{v} = 0$, robna integrala na desni strani en. (38) preoblikujemo, kar se kaže v končni obliki singularne robne integralske predstavitev kinematike prostorskega toka:

$$c(\xi)\vec{v}(\xi, t_F) + \alpha \int_{\Gamma} \int_{t_{F-1}}^{t_F} (\vec{\nabla} u^* \cdot \vec{n}) \vec{v} dt d\Gamma = \alpha \int_{\Gamma} \int_{t_{F-1}}^{t_F} (\vec{\nabla} u^* \times \vec{n}) \times \vec{v} dt d\Gamma + \alpha \int_{\Omega} \int_{t_{F-1}}^{t_F} (\vec{\omega} \times \vec{\nabla} u^*) dt d\Omega + \int_{\Omega} \vec{v}_{F-1} u_{F-1}^* d\Omega \quad (40)$$

ali tudi v zgoščenem simbolnem zapisu za krožno kombinacijo indeksov $ijkij = 12312$:

$$\begin{aligned} c(\xi)v_i(\xi, t_F) + \alpha \int_{\Gamma} \int_{t_{F-1}}^{t_F} v_i \frac{\partial u^*}{\partial n} dt d\Gamma &= \alpha \int_{\Gamma} \int_{t_{F-1}}^{t_F} v_k \left(\frac{\partial u^*}{\partial x_k} n_i - \frac{\partial u^*}{\partial x_i} n_k \right) dt d\Gamma \\ &- \alpha \int_{\Gamma} \int_{t_{F-1}}^{t_F} v_j \left(\frac{\partial u^*}{\partial x_i} n_j - \frac{\partial u^*}{\partial x_j} n_i \right) dt d\Gamma + \alpha \int_{\Omega} \int_{t_{F-1}}^{t_F} \omega_j \frac{\partial u^*}{\partial x_k} dt d\Omega - \alpha \int_{\Omega} \int_{t_{F-1}}^{t_F} \omega_k \frac{\partial u^*}{\partial x_j} dt d\Omega + \int_{\Omega} v_{i,F-1} u_{F-1}^* d\Omega \end{aligned} \quad (41)$$

Kinematika ravninskega toka je podana z:

$$c(\xi)v_i(\xi, t_F) + \alpha \int_{\Gamma} \int_{t_{F-1}}^{t_F} v_i \frac{\partial u^*}{\partial n} dt d\Gamma = \alpha \int_{\Gamma} \int_{t_{F-1}}^{t_F} v_j \frac{\partial u^*}{\partial t} dt d\Gamma - \alpha e_{ij} \int_{\Omega} \int_{t_{F-1}}^{t_F} \omega \frac{\partial u^*}{\partial x_j} dt d\Omega + \int_{\Omega} v_{i,F-1} u_{F-1}^* d\Omega \quad (42)$$

Enačba (41) je popolnoma ustrezna kontinuitetni oziroma omejitveni enačbi in definiciji vrtinčnosti ter podaja kinematiko nestisljive tekočine v integralski obliki. Hitrostni robni pogoji so vključeni v robnih integralih, medtem ko je z območnim integralom zajet vpliv vrtinčnega polja na razvoj hitrostnega polja. Zadnji območni integral upošteva vpliv začetnih hitrostnih pogojev nepravega prehodnega pojava. V en. (42) se pojavljata normalni in tangentni odvod osnovne rešitve $\partial u^*/\partial n$ in $\partial u^*/\partial t$, kar je pomembna razlika proti en. (39), kjer sta osnovna rešitev in njen normalni odvod, u^* in $\partial u^*/\partial n$. Pri izračunu robnih vrednosti funkcij polja moramo uporabiti normalno oziroma tangentno obliko vektorske enačbe (40), [7].

Robne vrednosti vrtinčnosti so v integralski obliki zajete v območnem integralu. Izračun robnih vrednosti vrtinčnosti zaradi zapisu nesingularnega implicitnega sistema terja tangentno obliko vektorske enačbe (40).

$$\begin{aligned} c(\xi)\vec{n}(\xi) \times \vec{v}(\xi, t_F) + \vec{n}(\xi) \times \alpha \int_{\Gamma} \int_{t_{F-1}}^{t_F} (\vec{\nabla} u^* \cdot \vec{n}) \vec{v} dt d\Gamma &= \\ \vec{n}(\xi) \times \alpha \int_{\Gamma} \int_{t_{F-1}}^{t_F} (\vec{\nabla} u^* \times \vec{n}) \times \vec{v} dt d\Gamma + \vec{n}(\xi) \times \alpha \int_{\Omega} \int_{t_{F-1}}^{t_F} (\vec{\omega} \times \vec{\nabla} u^*) dt d\Omega + \vec{n}(\xi) \times \alpha \int_{\Omega} \vec{v}_{F-1} u_{F-1}^* d\Omega & \end{aligned} \quad (43)$$

4.2 Integralska predstavitev kinetike

Za zapis kinetike toka viskoelastične tekočine v integralski obliki moramo upoštevati parabolično

One of the most important issues in the numerical modeling of incompressible flow phenomena is to obtain a divergence-free final solution both for the velocity field and for the vorticity conservation. In the case of equations (36) or (38) it can be easily shown that solutions where none of the divergences are zero are permitted [9]. Thus, it is possible to conclude that Eq. (38) does not generally represent the kinematics of incompressible fluid flow. By using additional compatibility and restriction conditions for the velocity and vorticity fields, $\vec{\omega} = \text{rot } \vec{v}$ and $\text{div } \vec{v} = 0$, boundary integrals on the right-hand side of Eq. (38) are rewritten, resulting in the final singular boundary integral statement of the kinematics of spatial flow:

or in the compact symbol notation for the cyclic combination of: $ijkij = 12312$:

$$\alpha \int_{\Gamma} \int_{t_{F-1}}^{t_F} v_k \left(\frac{\partial u^*}{\partial x_k} n_i - \frac{\partial u^*}{\partial x_i} n_k \right) dt d\Gamma - \alpha \int_{\Gamma} \int_{t_{F-1}}^{t_F} v_j \left(\frac{\partial u^*}{\partial x_i} n_j - \frac{\partial u^*}{\partial x_j} n_i \right) dt d\Gamma + \alpha \int_{\Omega} \int_{t_{F-1}}^{t_F} \omega_j \frac{\partial u^*}{\partial x_k} dt d\Omega - \alpha \int_{\Omega} \int_{t_{F-1}}^{t_F} \omega_k \frac{\partial u^*}{\partial x_j} dt d\Omega + \int_{\Omega} v_{i,F-1} u_{F-1}^* d\Omega$$

The kinematics of planar fluid motion is given by:

Equation (41) is equivalent to the continuity equation, also recognized as the restriction equation and the vorticity definition expressing the kinematics of general incompressible fluid flow in the integral form. Velocity boundary conditions are incorporated into boundary integrals, while in domain integrals the influence of the vorticity field on the developing velocity field is given. The last domain integral takes into account the influence of the initial velocity conditions of false transient phenomena. In Eq. (42) the normal and tangential derivatives of the fundamental solution, $\partial u^*/\partial n$ and $\partial u^*/\partial t$, are employed, an important difference in comparison to Eq. (39), where the fundamental solution and the normal derivative of the fundamental solution, u^* and $\partial u^*/\partial n$, are used. To compute the boundary values of the field functions, the normal or tangential form of vector Eq. (40), [7], is required.

The boundary vorticity values are expressed in integral form within the domain integral. When the unknowns are the boundary vorticities one has to use the tangential component of vector Eq. (40) because of the nonsingular implicit system of equations

4.2 Integral representation of flow kinetics

Considering the kinetics of viscoelastic fluid flow in an integral representation one has to take into

difuzivno-konvektivno naravo prenosne enačbe vrtinčnosti. Z uporabo linearnega paraboličnega difuzivnega diferencialnega operatorja:

$$L[\cdot] = \nu_0 \frac{\partial^2(\cdot)}{\partial x_j \partial x_j} - \frac{\partial(\cdot)}{\partial t} \quad (44)$$

prenosno enačbo vrtinčnosti (33) zapišemo v obliki nehomogene parabolične difuzivne enačbe:

$$L[\omega] + b = \nu_0 \frac{\partial^2 \omega}{\partial x_j \partial x_j} - \frac{\partial \omega}{\partial t} + b = 0 \quad (45)$$

z naslednjim pripadajočim integralskim stavkom, zapisanim za časovni korak $\Delta t = t_F - t_{F-1}$:

$$c(\xi)\omega(\xi, t_F) + \nu_0 \int_{\Gamma} \int_{t_{F-1}}^{t_F} \omega \frac{\partial u^*}{\partial n} dt d\Gamma = \nu_0 \int_{\Gamma} \int_{t_{F-1}}^{t_F} \frac{\partial \omega}{\partial n} u^* dt d\Gamma + \int_{\Omega} \int_{t_{F-1}}^{t_F} b u^* dt d\Omega + \int_{\Omega} \omega_{F-1} u_{F-1}^* d\Omega \quad (46)$$

kjer je u^* difuzivna osnovna rešitev, podana z en. (35). Območni integral nehomogenega nelinearnega prispevka b :

$$b = -\frac{\partial v_j \omega}{\partial x_j} + \frac{1}{\rho_0} e_{ij} g_j \frac{\partial \rho}{\partial x_i} + \frac{1}{\rho_0} e_{ij} \frac{\partial^2 \tau_{jk}^e}{\partial x_i \partial x_k} \quad (47)$$

vsebuje konvekcijo, vzgonske in elastične učinke, tako da velja naslednji zapis kinetike vrtinčnosti v integralski obliki:

$$\begin{aligned} c(\xi)\omega(\xi, t_F) + \nu_0 \int_{\Gamma} \int_{t_{F-1}}^{t_F} \omega \frac{\partial u^*}{\partial n} dt d\Gamma &= \nu_0 \int_{\Gamma} \int_{t_{F-1}}^{t_F} \frac{\partial \omega}{\partial n} u^* dt d\Gamma - \int_{\Gamma} \int_{t_{F-1}}^{t_F} \omega v_n u^* dt d\Gamma + \int_{\Omega} \int_{t_{F-1}}^{t_F} \omega v_j \frac{\partial u^*}{\partial x_j} dt d\Omega \\ &+ e_{ij} \frac{1}{\rho_0} \int_{\Gamma} \int_{t_{F-1}}^{t_F} n_i g_j \rho u^* dt d\Gamma - e_{ij} \frac{1}{\rho_0} \int_{\Omega} \int_{t_{F-1}}^{t_F} g_j \rho \frac{\partial u^*}{\partial x_i} dt d\Omega + e_{ij} \frac{1}{\rho_0} \int_{\Gamma} \int_{t_{F-1}}^{t_F} \frac{\partial \tau_{jk}^e}{\partial x_k} n_i u^* dt d\Gamma \\ &- e_{ij} \frac{1}{\rho_0} \int_{\Omega} \int_{t_{F-1}}^{t_F} \frac{\partial \tau_{jk}^e}{\partial x_k} \frac{\partial u^*}{\partial x_i} dt d\Omega + \int_{\Omega} \omega_{F-1} u_{F-1}^* d\Omega \end{aligned} \quad (48)$$

Iz en. (48) je razvidna popolna podobnost med prenosom vrtinčnosti v viskoelastični tekočini in prenosom vrtinčnosti v toku newtoniske viskozne tekočine z izjemo dodatnega elastičnega prispevka, ki deluje kot močno nelinearni izvirni člen.

Singularno robno integralsko predstavitev toplotne prenosne enačbe izpeljemo enako kakor izpeljavo vrtinčne enačbe, tako da velja integralski stavek:

$$\begin{aligned} c(\xi)T(\xi, t_F) + a_0 \int_{\Gamma} \int_{t_{F-1}}^{t_F} T \frac{\partial u^*}{\partial n} dt d\Gamma &= a_0 \int_{\Gamma} \int_{t_{F-1}}^{t_F} \frac{\partial T}{\partial n} u^* dt d\Gamma - \int_{\Gamma} \int_{t_{F-1}}^{t_F} T v_n u^* dt d\Gamma \\ &+ \int_{\Omega} \int_{t_{F-1}}^{t_F} T v_j \frac{\partial u^*}{\partial x_j} dt d\Omega + \int_{\Omega} T_{F-1} u_{F-1}^* d\Omega \end{aligned} \quad (49)$$

4.3 Integralska predstavitev tlačne enačbe

Tlačna en. (29) je eliptična Poissonova enačba, tako da uporabimo linearni eliptični Laplacev diferencialni operator:

$$L[\cdot] = \frac{\partial^2(\cdot)}{\partial x_i \partial x_i} \quad (50)$$

kar se izraža v zapisu:

account the parabolic diffusion-convection character of the vorticity transport equation. Since only the linear parabolic diffusion differential operator is employed, i.e.:

the vorticity equation (33) can be formulated as a nonhomogenous parabolic diffusion equation as follows:

with the following corresponding integral representation written in a time-increment form for a time step $\Delta t = t_F - t_{F-1}$:

where u^* is the parabolic diffusion fundamental solution given by Eq. (35). The domain integral of the non-homogenous nonlinear contribution b , represented as:

includes the convection, the bouyancy force effects, and the viscoelastic effects. Thus the final integral statement reads as:

Eq. (48) shows the analogy between the vorticity transport in the viscoelastic fluid and the vorticity transport in viscous, Newtonian motion, with the only difference in the extra viscoelastic contribution acting as a highly nonlinear source term.

By applying a similar procedure to the heat-transport equation, one derives the following integral statement:

4.3 Integral representation of the pressure equation

The pressure Eq. (29) is recognized as an elliptic Poisson equation, thus employing the linear elliptic Laplace differential operator:

the following can be stated:

$$L[p] + b = \frac{\partial^2 p}{\partial x_i \partial x_i} + b = 0 \quad (51)$$

medtem ko je pripadajoča singularna robna integralska tlačna predstavitev podana s stavkom:

$$c(\xi)p(\xi) + \int_{\Gamma} p \frac{\partial u^*}{\partial n} d\Gamma = \int_{\Gamma} \frac{\partial p}{\partial n} u^* d\Gamma + \int_{\Omega} bu^* d\Omega \quad (52)$$

kjer je u^* Laplaceova osnovna rešitev, npr. rešitev enačbe:

$$\frac{\partial^2 u^*}{\partial x_i \partial x_i} + \delta(\xi, s) = 0 \quad (53)$$

Za ravninsko geometrijo velja rešitev:

$$u^* = \frac{1}{2\pi} \ln\left(\frac{1}{r}\right) \quad (54)$$

Z izenačitvijo navidezno prostorninskih sil:

For planar geometry the following solution is suitable:

$$b = -\frac{\partial f_i}{\partial x_i} \quad (55)$$

izpeljemo integralsko odvisnost:

By equating pseudo-body forces with the expression:

$$c(\xi)p(\xi) + \int_{\Gamma} p \frac{\partial u^*}{\partial n} d\Gamma = \int_{\Gamma} \frac{\partial p}{\partial n} u^* d\Gamma - \int_{\Omega} \frac{\partial f_i}{\partial x_i} u^* d\Omega \quad (56)$$

Z Gaussovim divergenčnim stavkom območni integral v en. (56) preoblikujemo kot:

Using the Gauss divergence theorem the domain integral in eq. (56) is rewritten as:

$$\int_{\Omega} \frac{\partial f_i}{\partial x_i} u^* d\Omega = \int_{\Gamma} f_i n_i u^* d\Gamma - \int_{\Omega} f_i \frac{\partial u^*}{\partial x_i} d\Omega \quad (57)$$

ker pa je $\partial p / \partial n = \vec{f} \cdot \vec{n}$, velja končna oblika tlačnega integralskega stavka:

because the relation $\partial p / \partial n = \vec{f} \cdot \vec{n}$, the final form of the pressure integral statement is obtained:

$$c(\xi)p(\xi) + \int_{\Gamma} p \frac{\partial u^*}{\partial n} d\Gamma = \int_{\Omega} f_i \frac{\partial u^*}{\partial x_i} d\Omega \quad (58)$$

kjer je vektor f_i podan za prostorski tok z en. (27) in za ravninsko gibanje z en. (29).

where vector f_i for the spatial flow is given by eq. (27) and for planar flow by Eq. (29).

5 RAČUNSKA SHEMA

Singularne robnoobmočne integralske enačbe lahko rešimo za neznane funkcije polja le približno v smislu ustreznegra numeričnega modela, s katerim integralske enačbe predelamo v pripadajoči sistem algebrajskih enačb. Osnova modela robnih elementov je diskretizacija roba z robnimi elementi in območja rešitve z notranjimi celicami [10]. Ker je za utežno funkcijo izbrana Greenova osnovna rešitev, z robo diskretizacijo v celoti zajamemo linearni del rešitve (difuzijo), medtem ko z notranjo delitvijo na celice upoštevamo nelinearne prispevke prenosnega pojava. V prispevku so uporabljeni daljščni kvadratni zvezni robeni elementi in četverokotne kvadratne zvezne notranje celice.

V računskem postopku iskanja približne rešitve predstavlja kinematika in kinetika prenosnega pojava vezan nelinearni sistem. V primeru splošnega časovno odvisnega pojava izračunamo najprej na temelju znanih začetnih vrednosti funkcij polja nove približke vrtinčnega polja z rešitvijo en. (48). Z novimi območnimi

while the corresponding singular integral pressure representation is given by:

where u^* is the Laplace fundamental solution, being the solution of the equation:

For planar geometry the following solution is suitable:

By equating pseudo-body forces with the expression:

the integral statement is derived:

5 COMPUTATIONAL SCHEME

If one wants to solve singular, boundary-domain, integral equations to obtain values of field functions in the computational domain one first has to transform the derived integral equations into their discrete algebraic forms. The key to this is the partitioning of the computational external boundary into boundary elements and the interior domain into domain cells [10]. Use of the Green fundamental solution results in boundary discretization of the linear part of the solution (diffusion), while internal cells take care of the nonlinear contribution of the transport phenomena. In this paper, quadratic interpolation functions were used in the case of boundary elements and internal cells in the case of domain.

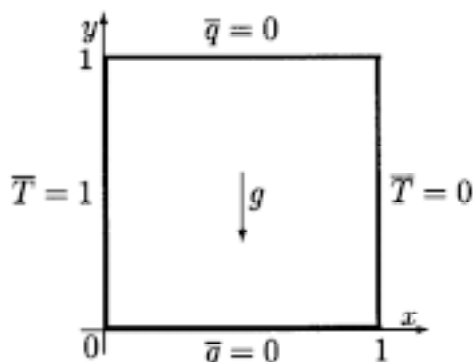
The kinematics and kinetics of the fluid-flow motion can be seen as two intertwined problems in a nonlinear system of equations. For general time-dependent flows using known information about the motion at an instant time level, new vorticity values for a subsequent time level are determined by solving eq. (48). With this new domain, vorticity values corresponding to

vrednostmi vrtinčnosti kinetike toka izračunamo nove robne vrednosti vrtinčnosti z rešitvijo kinematike en. (43). Ta izračun je ključnega pomena za ohranitev solenoidnosti hitrostnega in vrtinčnega polja. Sledi izrecen izračun hitrosti v območju. Če obravnavamo neizotermne tokove, pri katerih so vzgonski učinki pomembni, so vse tri enačbe, tj. kontinuitetna, vrtinčna in energijska, vezane v močno nelinearen sistem, ki ga lahko razrešimo le iterativno. Za viskoelastične tekočine velja, da moramo v nelinearno shemo vključiti še izračun napetostnega tenzorja, skladno z reološkim modelom. Tlačno polje določimo zunaj nelinearne sheme na podlagi vseh znanih funkcij polja z rešitvijo en. (58).

6 NUMERIČNI REZULTATI

6.1 Naravna konvekcija

V prvem numeričnem primeru smo preučili naravno konvekcijo viskoelastične tekočine v zaprti kotanji. Kot standardni testni primer CFD je problem gibanja newtonske tekočine zaradi vzgonskih sil predložil že De Vahl Davis sodelavci ([2] in [3]).



Sl. 1. Naravna konvekcija v zaprti kotanji. Geometrija in robni pogoji.
Fig. 1. Natural convection in a closed cavity. Geometry and boundary conditions.

Kotanja je popolnoma napolnjena z nestisljivo viskoelastično tekočino. Uporabljena konstitutivna modela sta v prvem primeru kvazilinearni Maxwellov model (model A) in v drugem premeru zgornje konvektivni Maxwellov model (model B), ki sta podrobno opisana v poglavju 3.

Zgornja in spodnja stena kotanje sta izolirani, medtem ko sta leva in desna stena ogreti na različno temperaturo. Zaradi temperaturne razlike obstaja toplotni tok v tekočini. Ker je gostota tekočine odvisna od temperature, se pojavi vzgonske sile, ki poganjajo tekočino. Ob topli steni se tekočina dviguje, ob hladni spušča. Hitrost gibanja newtonske tekočine je funkcija Rayleighevega števila $Ra = g\beta(T_i - T_k)L^3/a_0\nu$. V našem primeru smo izbrali $Ra = 10^3$. Tok newtonske tekočine ($\lambda_1 = 0$) smo primerjali z nenewtonskimi tokovi za vrednosti napetostnega sprostivenega časa $\lambda_1 = 0,06, 0,07$ in $0,08$. Masna

boundary vorticity values are determined by solving the flow kinematics Eq. (43). This part of the computation is of crucial importance for preserving the solenoidality of the velocity and vorticity fields, which is followed by an explicit computation of domain velocities. In the case of nonisothermal flows, where the buoyance forces are important, all three equations, such as the continuity, vorticity and energy equations, are coupled into a highly nonlinear system, which can be solved only iteratively. For viscoelastic fluids, an additional nonlinearity is introduced by computing the components of the stress tensor in accordance with the rheological model employed. The pressure field is determined outside the nonlinear scheme on the basis of all known field functions by solving Eq. (58).

6 NUMERICAL SOLUTION

6.1 Natural convection

As a first numerical example, the natural convection of a viscoelastic fluid in a closed cavity is examined. The problem has been analyzed by De Vahl Davis et al. ([2] and [3]) as one of the standard test cases of Newtonian viscous fluid flows in CFD.

A cavity is filled with an incompressible viscoelastic fluid. Two different rheological models are employed: the quasilinear Maxwell model in case A and the upper-convected Maxwell model in case B. Both are described in detail in section 3.

The top and bottom walls are insulated, while the left-hand and right-hand walls are heated to different temperatures. Due to the temperature difference a heat flow occurs through the fluid. Because the density of the fluid depends on the temperature, the fluid starts moving upward at the hot wall due to buoyancy, and downward at the cold wall. The velocity of the fluid depends on the Rayleigh number $Ra = g\beta(T_i - T_k)L^3/a_0\nu$. In our case $Ra = 10^3$ was selected. The Newtonian fluid flow ($\lambda_1 = 0$) was compared to the non-Newtonian flow for different values of the relaxation time parameter $\lambda_1 =$

gostota je podana z enačbo stanja $\rho = \rho_0(1+\beta T)$ idealnega plina.

0.06, 0.07 and 0.08. The mass density is given by the equation of state $\rho = \rho_0(1+\beta T)$.



Sl. 2. Naravna konvekcija nenewtoniske viskoelastične tekočine modelirana z zgornje konvektivnim Maxwellovim reološkim modelom ($\lambda_1=0,07$); vektorji hitrosti (levo), tokovnice (sredina) in izolinije vrtinčnosti (desno)

Fig. 2. Natural convection of non-Newtonian viscoelastic fluid modeled with upper-conveected Maxwell rheological model ($\lambda_1=0.07$); velocity vectors (left), streamlines (middle), and vorticity lines (right)

Preglednica 1. Primerjava vrednosti \overline{Nu} števila med newtonskega tekočino in različnimi modeli nenewtoniske tekočine

Table 1. Comparison of \overline{Nu} number for Newtonian fluid flow and different models of non-Newtonian fluid flow

λ_1	Davis	MRE - A			MRE - B		
	0	0,6	0,7	0,8	0,6	0,7	0,8
\overline{Nu}	1,117	1,136	1,134	1,132	1,176	1,162	/

Geometrija problema in robni pogoji so prikazani na sliki 1. Računska mreža je sestavljena iz 80 robnih elementov in 400 notranjih celic, kar pomeni mrežo 20×20 celic z razmerjem 6 med najdaljšim in najkrajšim elementom. Vse izračune smo izvedli kot ustaljene, pri čemer smo prehodni pojav simulirali z zelo velikim časovnim korakom ($\Delta t = 10^{16}$). Podsprostitev smo definirali s podsprostivščim parametrom ϑ , ki je znašal v primeru simulacije newtonskega toka $\vartheta = 0,001$ in v primeru izračuna nenewtonskih tokov $\vartheta = 0,0001$. Konvergenčni kriterij je vedno predstavljala napaka v velikosti $= 10^{-6}$.

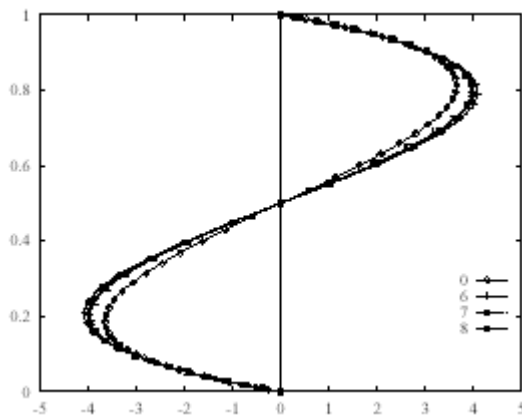
Slika 2 prikazuje vektorsko polje hitrosti, tokovnice in izočrte vrtinčnosti za zgornje konvektivni Maxwellov reološki model (B) pri vrednosti parametra $\lambda_1 = 0,07$. Slike 3, 4, 5 in 6 prikazujejo hitrostne profile v_y vz dolž vodoravnih črte in hitrostne profile v_x vz dolž navpičnih črte skozi geometrijsko središče kotanje. Izvedena je primerjava newtonske primerjalne rešitve MRE na gostoti mreže 32×32 , ki se odlično ujema z rešitvijo Davisa ([2] in [3]), z nenewtonskimi rešitvami MRE na že omenjeni računski mreži 20×20 .

Na slikah 3 in 4 je nenewtoniska tekočina modelirana kot navidezlinearna (A), na slikah 5 in 6 pa so prikazani rezultati zgornje konvektivnega Maxwellovega modela viskoelastične tekočine (B). Opazimo razmeroma velik vpliv elastičnosti tekočine

The geometry and boundary conditions of the problem are shown in Fig. 1. The computational mesh is composed of 80 boundary elements and 400 internal cells, i.e. 20×20 cells with a ratio of 6 between the longest and the shortest element. All the simulations were performed as steady with the transient phenomenon simulated using an extremely large time step ($\Delta t = 10^{16}$). The underrelaxation parameter ϑ (in the case of a temperature computation defined by $T^{+1} = \vartheta T^{+1} + (1-\vartheta)T^t$ and analogous for other field functions) was set to $\vartheta = 0.001$ in the case of Newtonian flow and $\vartheta = 0.0001$ in case of non-Newtonian flows. The convergence criterion was selected as $\varepsilon = 10^{-6}$.

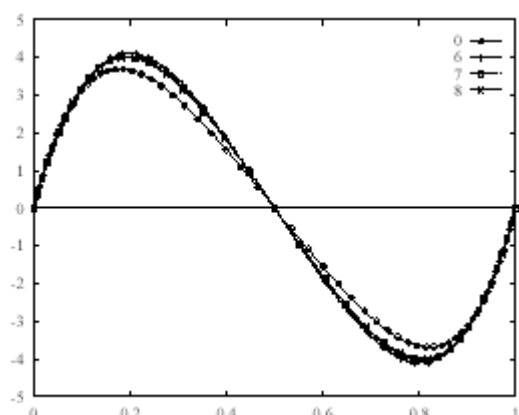
Fig. 2 shows the velocity vectors, the streamlines, and the vorticity lines for the upper-conveected Maxwell rheological model (B) for the relaxation-time parameter being fixed at $\lambda_1 = 0.07$. Figs. 3, 4, 5, and 6 show velocity profiles v_y along a horizontal line and velocity profiles v_x along a vertical line, through the geometric center of the cavity. The comparison between a BEM reference solution obtained on mesh density 32×32 , which is in excellent agreement with the Davis solution ([2] and [3]), and BEM non-Newtonian solutions obtained on mesh density 20×20 is performed.

On Figs. 3 and 4 the non-Newtonian fluid is modeled as quasilinear (A), while in Figs. 5 and 6 the upper-conveuted Maxwell model (B) is used. It is easy to see a relatively strong influence of the



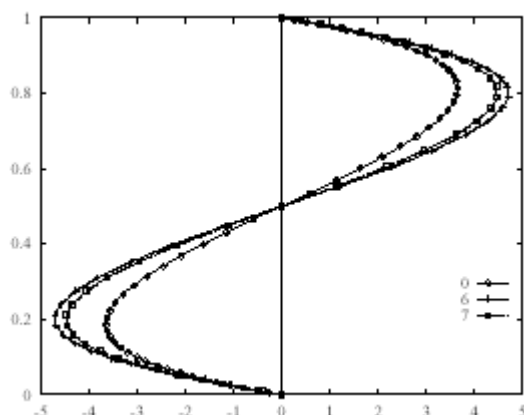
Sl. 3. Nenewtonska tekočina kot Maxwellova navidezlinearna viskoelastična tekočina (A). Hitrostni profili v_x vzdolž navpične črte skozi geometrijsko središče kotanje.

Fig. 3. Non-Newtonian fluid as Maxwell quasilinear viscoelastic fluid (A). Velocity profiles v_x along a vertical line through the center of cavity.
(0 : $\lambda_i=0$; 6 : $\lambda_i=0,06$; 7 : $\lambda_i=0,07$ in/and 8 : $\lambda_i=0,08$)



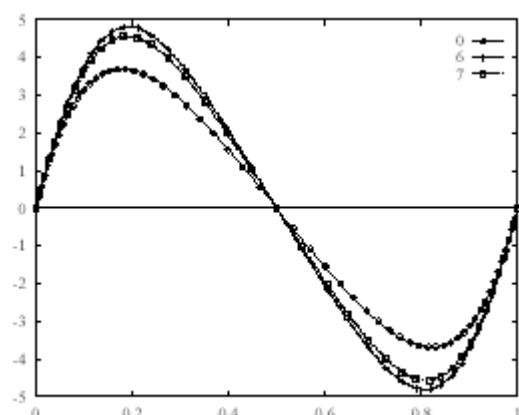
Sl. 4. Nenewtonska tekočina kot Maxwellova navidezlinearna viskoelastična tekočina (A). Hitrostni profili v_y vzdolž vodoravne črte skozi geometrijsko središče kotanje.

Fig. 4. Non-Newtonian fluid as Maxwell quasilinear viscoelastic fluid (A). Velocity profiles v_y along a horizontal line through the center of cavity.
(0 : $\lambda_i=0$; 6 : $\lambda_i=0,06$; 7 : $\lambda_i=0,07$ in/and 8 : $\lambda_i=0,08$)



Sl. 5. Nenewtonska tekočina kot Maxwellova zgornje konvektivna viskoelastična tekočina (B). Hitrostni profili v_x vzdolž navpične črte skozi geometrijsko središče kotanje.

Fig. 5. Non-Newtonian fluid as Maxwell upper-convedted viscoelastic fluid (B). Velocity profiles v_x along a vertical line through the center of cavity.
(0 : $\lambda_i=0$; 6 : $\lambda_i=0,06$ in/and 7 : $\lambda_i=0,07$)



Sl. 6. Nenewtonska tekočina kot Maxwellova zgornje konvektivna viskoelastična tekočina (B). Hitrostni profili v_y vzdolž vodoravne črte skozi geometrijsko središče kotanje.

Fig. 6. Non-Newtonian fluid as Maxwell upper-convedted viscoelastic fluid (B). Velocity profiles v_y along a horizontal line through the center of cavity.
(0 : $\lambda_i=0$; 6 : $\lambda_i=0,06$ in/and 7 : $\lambda_i=0,07$)

v primeru zgornje konvektivnega reološkega modela. V reološkem modelu (12) se ob Stokesovem odvodu dodatnega napetostnega tenzorja oziroma tenzorja gostote toka gibalne količine pojavi dodaten člen, ki opravlja prenos gibalne količine na način, ki ga lahko enačimo z raztezno - obračalnim mehanizmom v prenosni enačbi vrtinčnosti (21).

V preglednici 1 je prikazana primerjava vrednosti povprečnega Nusseltovega števila \bar{Nu} za

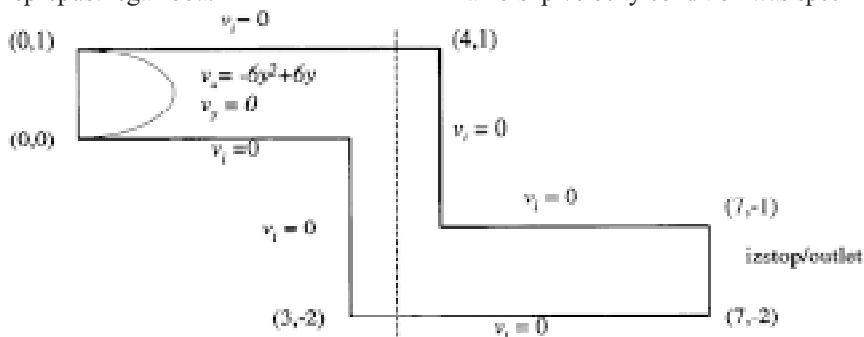
viscoelasticity in the case of the upper-convedted rheological model. For the rheological model (12), not only the Stokes derivative of the extra-stress tensor is acting, but also an extra term is employed, adding the momentum transport similar to the twisting and stretching mechanism of exchange in the vorticity transport equation (21).

Table 1 shows the comparison of the values of the average Nusselt number \bar{Nu} for the Newtonian

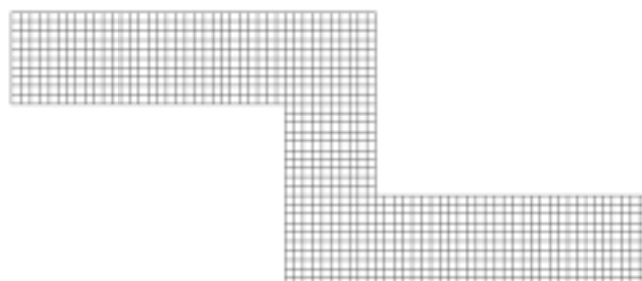
newtonsko tekočino in za različne vrednosti napetostnega relaksacijskega časa (λ_i) pri izbranih Maxwellovih reoloških modelih nenewtonske tekočine.

6.2 Tok v kanalu oblike Z

Kot drugi numerični primer smo preučili tok viskoelastične tekočine v zavitem kanalu oblike Z. Uporabljeni reološki model je Maxwellov zgornje konvektivni model (B). Izbran testni primer je zapletena kombinacija vstopno - izstopnega problema, ostrih robov in dodatnih nelinearnosti zaradi modeliranja toka nenewtonske tekočine. Slika 7 prikazuje geometrijsko obliko kanala z robnimi pogoji. Pri vstopu v kanal smo predpisali razviti profil laminarnega toka s povprečno hitrostjo 1,0 m/s ($\bar{v}_{in} = 1,0 \text{ m/s}$). Pri izstopu smo definirali izstopne robne pogoje. Trdne stene zaznamujejo brezzdrsni robni pogoji neprepustnega roba.



Sl. 7. Kanal oblike Z. Geometrija in robni pogoji
Fig. 7. Flow in Z channel. Geometry and boundary conditions



Sl. 8. Računska mreža pri modeliranju toka viskoelastične tekočine v kanalu oblike Z
Fig. 8. Computational mesh for simulation of viscoelastic fluid in Z channel

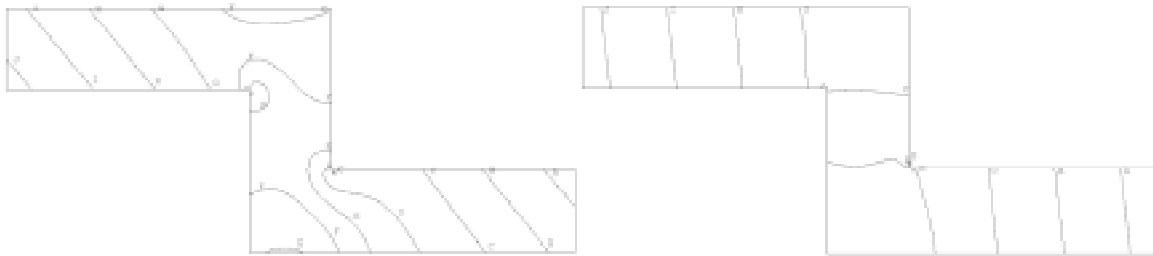


Sl. 9. Tok nenewtonske viskoelastične tekočine v kanalu oblike Z modelirane z zgornje konvektivnim Maxwellovim reološkim modelom ($\lambda_i=0,06$); tokovnice (levo) in izočrte vrtinčnosti (desno)
Fig. 9. Non-Newtonian viscoelastic fluid flow in Z channel. Upper-convedted Maxwell rheological model with ($\lambda_i=0.06$); streamlines (left) and vorticity lines (right)

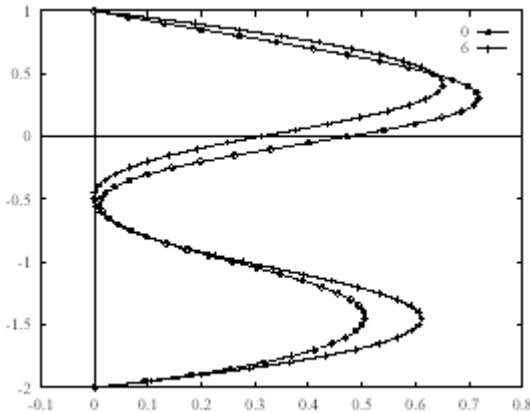
fluid and for different values of the relaxation time (λ_i) in the case of the Maxwell non-Newtonian rheological models.

6.2 Flow in Z channel

As a second numerical example, the flow of a viscoelastic fluid in a bent channel with a Z shape is examined. The Maxwell upper-convedted rheological model (B) was selected. Flow in a bent channel represents a complicated combination of the inlet-outlet problem, sharp edges, and extra nonlinearities as result of viscoelastic non-Newtonian fluid flow. The geometry of the channel with the boundary conditions prescribed is shown in Fig. 7. At the inlet to the channel, a laminar parabolic velocity profile with an average velocity of 1.0 m/s ($\bar{v}_{in} = 1.0 \text{ m/s}$) was prescribed. At the outlet, outlet velocity conditions were given. At the solid walls a no-slip velocity condition was specified.



Sl. 10. Primerjava tlačnih polj v kanalu oblike Z. 0 : $\lambda_1=0$ (desno) in 6 : $\lambda_1=0,06$ (levo)
Fig. 10. Comparison of pressure fields in Z channel. 0 : $\lambda_1=0$ (right) and 6 : $\lambda_1=0,06$ (left)



Sl. 11. Profil hitrosti v_x vzdolž navpičnice skozi središčno točko geometrije kanala

Fig. 11. Velocity profile v_x along a vertical line through the center of the channel
(0 : $\lambda_1=0$ in/and 6 : $\lambda_1=0,06$)

Enakomerno računsko mrežo je sestavljalo 200 robnih elementov in 900 notranih celic. Prikazana je na sliki 8.

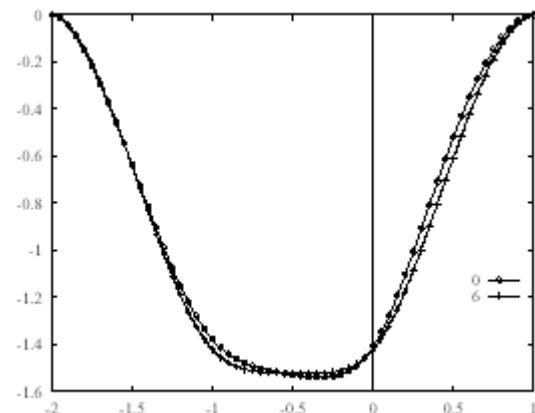
Reynoldsovo število in Weissenbergovo število sta definirani kot:

$$Re = \frac{\bar{v}_{out} L}{\nu} \quad (59)$$

$$We = \frac{\lambda_1 \bar{v}_{out}}{L} \quad (60)$$

kjer sta ν in λ_1 kinematična viskoznost tekočine in napetostni sprostivitveni čas ter je (\bar{v}_{out}) karakteristična hitrost (povprečna izstopna). Karakteristična linearna izmera L pomeni polovico višine izstopne odprtine. V skladu z navedenimi definicijami je tok v kanalu blizu Stokesovemu z vrednostjo Reynoldsovega števila $Re = 0,7$. Vrednost Weissenbergovega števila, odločilnega za konvergenco numeričnega algoritma, je znašala $We = 0,12$. Vse izračune smo ponovno izvedli kot ustaljene, pri čemer smo prehodni pojav simulirali z zelo velikim časovnim korakom ($\Delta t = 10^{16}$). Podsprostitev smo definirali s podsprostivtvenim parametrom ϑ , ki je znašal v primeru simulacije newtonskega toka $\vartheta = 0,01$ in v primeru nenewtonskega toka $\vartheta = 0,001$. Konvergenčni kriterij je bila kot vedno napaka v velikosti $\varepsilon = 10^{-6}$.

Slike 11 in 12 prikazujejo profile hitrosti v_x in v_y vzdolž navpičnice skozi središčno točko geometrijske



Sl. 12. Profil hitrosti v_y vzdolž navpičnice skozi središčno točko geometrije kanala

Fig. 12. Velocity profile v_y along a vertical line through the center of the channel
(0 : $\lambda_1=0$ in/and 6 : $\lambda_1=0,06$)

A uniform computational mesh consists of 200 boundary elements and 900 internal cells. It is shown in Fig. 8.

The Reynolds and Weissenberg numbers were defined according to convention as:

$$Re = \frac{\bar{v}_{out} L}{\nu} \quad (59)$$

$$We = \frac{\lambda_1 \bar{v}_{out}}{L} \quad (60)$$

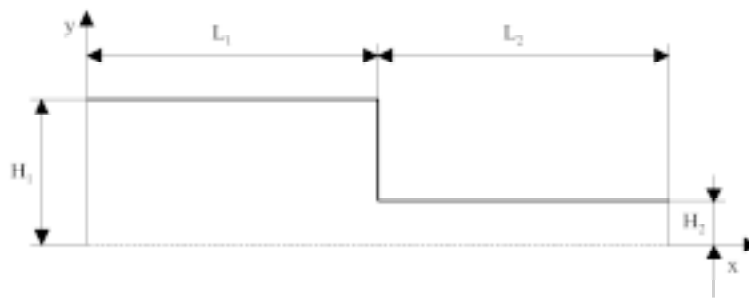
where ν and λ_1 are the fluid kinematic viscosity and the relaxation time, respectively, and (\bar{v}_{out}) is a characteristic velocity (average at the outlet). A characteristic linear dimension L is defined as half of the outlet opening. Throughout the channel, creeping flow was assumed with $Re = 0.7$. The value of the Weissenberg number, which is crucial for achieving the stability of the numerical algorithm according to the literature, was chosen to be $We = 0.12$. All the simulations were again performed as steady with a large time step ($\Delta t = 10^{16}$). Underrelaxation was defined with the underrelaxation parameter ϑ set to $\vartheta = 0.01$ in the case of Newtonian flow and $\vartheta = 0.001$ in the case of non-Newtonian flow. The convergence criterion was selected as $\varepsilon = 10^{-6}$.

Figs. 11 and 12 show the velocity profiles v_x and v_y along a vertical line through the center of the

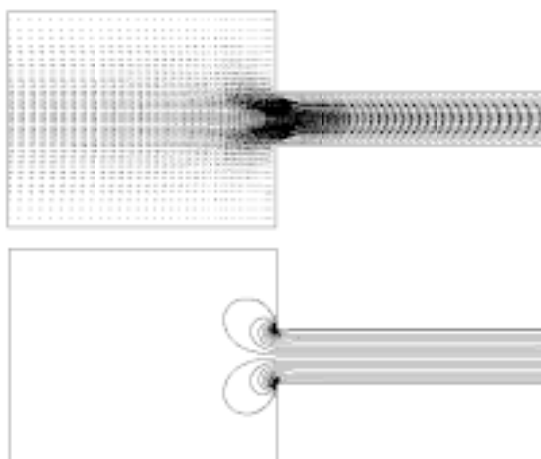
oblike kanala. Primerjamo tok newtonske tekočine ($\lambda_1 = 0$) s tokom viskoelastične tekočine (Maxwellov zgornje konvektivni model) pri vrednosti ($\lambda_1 = 0,06$). Slika 10 kaže primerjavo tlačnih polj omenjenih tokov.

6.3 Tok v simetričnem kanalu z nadaljnjo zožitvijo 4:1

Predstavljeni numerični algoritem smo testirali tudi na vstopno-izstopnem problemu toka viskoelastične tekočine v simetričnem kanalu z nadaljnjo zožitvijo 4:1, katerega geometrijska oblika je predstavljena na sliki 13.



Sli. 13. Kanal z nadaljnjo 4:1 zožitvijo
Fig. 13. Channel with a 4:1 abrupt contraction

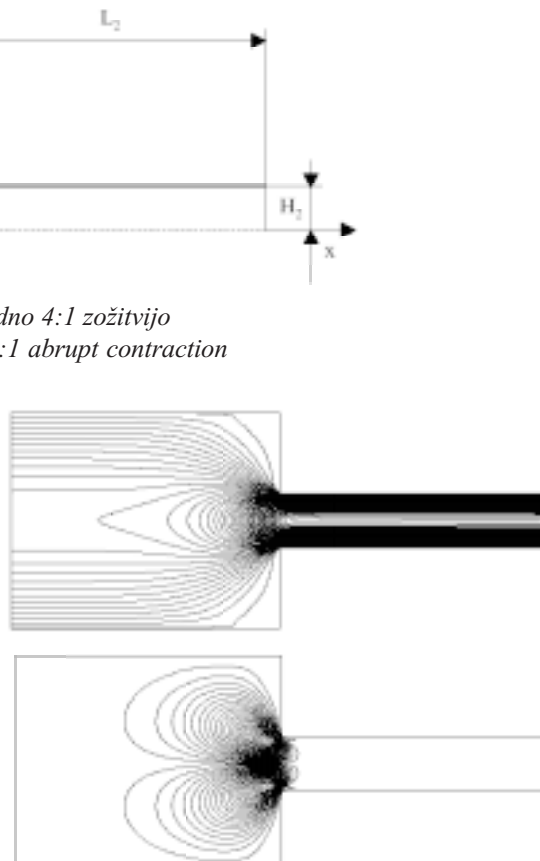


Sli. 14. Kanal z nadaljnjo 4:1 zožitvijo. Vektorji hitrosti (zgoraj) in vrtinčno polje (spodaj)
Fig. 14. Channel with a 4:1 abrupt contraction.
Velocity vectors (above) and vorticity field (below)

channel. A comparison of the Newtonian fluid flow ($\lambda_1 = 0$) and the non-Newtonian viscoelastic fluid flow (Maxwell upper-convected model) at ($\lambda_1 = 0,06$) is shown. Fig. 10 presents the pressure fields in both cases.

6.3 Flow in a 4:1 planar sudden-contracted channel

The developed numerical algorithm was tested for the test case of analysing the inflow-outflow viscoelastic fluid problem in a planar channel with a 4:1 sudden contraction. A detailed presentation of the flow geometry is given in fig. 13.



Sli. 15. Kanal z nadaljnjo 4:1 zožitvijo. Izocrite hitrosti v smeri koordinatne osi x (zgoraj) in izocrite hitrosti v smeri koordinatne osi y (spodaj)
Fig. 15. Channel with a 4:1 abrupt contraction.
Velocity lines in coordinate direction x (above) and velocity lines in coordinate direction y (below)

Oba dela kanala (vstopni in izstopni) merita v dolžino $L_1 = L_2 = 10H_2$, kar zadošča za popolno razvitje hitrostnega profila. Tokovne razmere v kanalu podobne geometrijske oblike so podrobno predstavljene v [6]. Izmera H_2 je določena kot polovica višine izstopnega kanala ($H_2 = 0,125$). Reynoldsovo število in Weissenbergovo število sta definirani enako kakor v prejšnjem primeru. Tok v kanalu je zelo blizu Stokesovemu z vrednostjo Reynoldsovega števila Re

The inlet and outlet lengths were both $L_1 = L_2 = 10H_2$ to ensure fully developed flows in these regions. The flow field in a channel of similar geometry is described in detail in [6]. The dimension H_2 is defined as the half-width of the downstream channel ($H_2 = 0,125$). The Reynolds and Weissenberg numbers are defined as in the previous case. Throughout the channel, almost creeping flow was assumed with $Re = 0.001$. The

$= 0,001$. Vrednosti Weisenbergovega števila smo spremenjali od $We = 6,4 \times 10^{-3}$ ($\lambda_1 = 0,1$) do $We = 51,2 \times 10^{-3}$ ($\lambda_1 = 0,8$), kar je podobno navedenemu v [1].

Za numerično modeliranje smo uporabili diskretizacijo, sestavljeno iz 560 neenakih notranjih celic, zgoščenih okoli ostrih vogalov pri zožitvi kanala. Pri vstopu v kanal smo predpisali razviti parabolični profil laminarnega toka s povprečno hitrostjo 0,002 m/s ($\bar{v}_m = 0,002 \text{ m/s}$). Ta vrednost ustreza izstopnemu paraboličnemu profilu z ($\bar{v}_{out} = 0,008 \text{ m/s}$). Na trdnih stenah smo predpisali brezdrsne hitrostne robne pogoje. Na začetku modeliranja ($t = 0$) je bilo računsko območje popolnoma napolnjeno z mirujočo tekočino. Ustaljeno stanje smo modelirali s časovnim korakom ($\Delta t = 10^{16}$), medtem ko je vrednost podsprostivitvenega parametra znašala $\vartheta = 0,01$. Konvergenčni kriterij smo nastavili na $\varepsilon = 10^{-6}$.

Slike 14 in 15 prikazujeta vektorsko polje hitrosti, polje vrtinčnosti ter izočrte hitrosti v koordinatnih smereh x in y v ustaljenem stanju viskoelastičnega toka $\lambda_1 = 0,8$ za $Re = 0,001$ in $We = 51,2 \times 10^{-3}$.

7 SKLEP

V prispevku je predstavljena metoda robnih elementov za modeliranje toka viskoelastične tekočine. Različni Maxwellovi modeli prikazujejo široko uporabnost MRE. Kljub dodatnim nelinearnim izvirnim členom razvita shema ohranja vse prednosti modeliranja nestisljivih viskoznih tokov z MRE [5]. Kot testni primer rabijo naravna konvekcija viskoelastične tekočine v zaprti kotanji, tok v kanalu oblike Z in tok v kanalu z nenadno zožitvijo 4 : 1. Na podlagi rezultatov ugotavljam, da je razvita shema stabilna in natančna.

Weissenberg number varied from $We = 6,4 \times 10^{-3}$ ($\lambda_1 = 0,1$) to $We = 51,2 \times 10^{-3}$ ($\lambda_1 = 0,8$), similar to [1].

The computational mesh used for the simulations consisted of 560 non-uniform internal cells refined around the sharp corner of the inlet to the exit channel. At the inlet to the main channel the laminar parabolic velocity profile with an average velocity of 0.002 m/s ($\bar{v}_m = 0,002 \text{ m/s}$) was prescribed corresponding to the outlet parabolic velocity profile with ($\bar{v}_{out} = 0,008 \text{ m/s}$). At the solid walls a no-slip velocity condition was specified. At the beginning of the simulation ($t = 0$) the computational domain was filled with quiescent fluid. The steady state was modeled with the time step ($\Delta t = 10^{16}$), and with the underrelaxation parameter set to $\vartheta = 0,01$. The convergence criterion was selected as $\varepsilon = 10^{-6}$.

Figs. 14 and 15 show the velocity vector field, the vorticity field and the velocity isolines in both coordinate directions x and y in the steady state of the viscoelastic non-Newtonian upper-conveyed Maxwell fluid flow $\lambda_1 = 0,8$ for $Re = 0,001$ and $We = 51,2 \times 10^{-3}$.

7 CONCLUSIONS

The boundary-domain integral approach to the solution of viscoelastic fluid motion problems is presented. Different Maxwell fluid models are used to show the applicability of the proposed BEM model. All the attractive features of the BEM model, based on the application of different fundamental solutions already established in viscous fluid dynamics, are preserved [5]. The numerical scheme is verified using test cases of a viscoelastic fluid's natural convection flow, viscoelastic flow through the Z channel, and a 4 : 1 abrupt-contraction-channel viscoelastic flow. The computational results show that the scheme is stable and accurate.

8 LITERATURA 8 REFERENCES

- [1] Aboubacar, M., M.F. Webster (2001) A cell-vertex finite volume/element method on triangles for abrupt contraction viscoelastic flows. *J. Non-Newtonian Fluid Mech.*, 98, 83-106.
- [2] Davis, G.D.V., I.P. Jones (1983) Natural convection in a square cavity: A comparison exercise. *Int. Jou. for Num. Meth. in Fluids.*, 3, 227-248.
- [3] Davis, G.D.V. (1983) Natural convection of air in a square cavity: A bench mark numerical solution. *Int. Jou. for Num. Meth. in Fluids.*, 3, 249-264.
- [4] Dou, H., N.P. Thien (1999) The flow of an Oldroyd-B fluid past a cylinder in a channel: adaptive viscosity vorticity (DAVSS- ω) formulation; *J. Non-Newtonian Fluid Mech.*, 87, 47-73.
- [5] Hriberšek, M., L. Škerget (1999) Fast boundary-domain integral algorithm for computation of incompressible fluid flow problems. *Int. J. Num. Meth. Fluids.*, 31, 891-907.
- [6] Oliveira, P.J., F.T. Pinho (1999) Plane contraction flows of upper convected Maxwell and Phan-Thien-Tanner fluids as predicted by a finite-volume method; *J. Non-Newtonian Fluid Mech.*, 88, 63-88.
- [7] Škerget, L., A. Alujević, C.A. Brebbia, G. Kuhn (1989) Natural and forced convection simulation using the velocity-vorticity approach. *Topics in Boundary Element Research.*, 5(4), 49-86.

- [8] Škerget, L., M. Hriberšek, G. Kuhn (1999) Computational fluid dynamics by boundary-domain integral method. *Int. J. Numer. Meth. Engng.*, 46, 1291-1311.
- [9] Wu, J.C. (1982) Problems of general viscous flow. Developments in BEM. *Elsevier Appl. Sci. Publ.*, 2(2).
- [10] Wrobel, L.C. (2002) The boundary element method. Vol. 1., Applications in thermo-fluids and acoustics. *Wiley*.

Naslov avtorjev: prof.dr. Leopold Škerget
dr. Matej Požarnik
Fakulteta za strojništvo
Univerza v Mariboru
Smetanova 17
2000 Maribor
leo@uni-mb.si
matej.pozarnik@uni-mb.si

Author's Address: Prof.Dr. Leopold Škerget
Dr. Matej Požarnik
Faculty of Mechanical Eng.
University of Maribor
Smetanova 17
2000 Maribor, Slovenia
leo@uni-mb.si
matej.pozarnik@uni-mb.si

Prejeto: 20.12.2002
Received:

Sprejeto: 31.1.2003
Accepted: